Neuroradiology (2003) 45: 773–779
DOI 10.1007/s00234-003-1001-5

F. Zhang
J. Xie
H. Han

MRI reveals changes in intracellular calcium in ischaemic areas of rabbit brain

Received: 20 February 2003
Accepted: 17 March 2003
Published online: 10 October 2003

F. Zhang · J. Xie · H. Han (✉)
Department of Radiology,
Peking University Third Hospital,
49 North Gardon Road,
100083 Peking, China
E-mail: mrifang@sina.com
Tel.: +86-10-64871676
Fax: +86-10-13681032578

Abstract Since calcium overload is thought to be important in ischaemic neuronal death, we have used a focal ischaemic model to determine the relationships between changes in intracellular calcium concentration ($[Ca^{2+}]_i$), apparent diffusion coefficient (ADC), and relative cerebral blood flow (rCBF). Focal cerebral ischaemia was induced in seven groups of six rabbits, by transorbital permanent occlusion of one middle cerebral artery (MCAo). Diffusion- and perfusion-weighted imaging was performed from 0.5 to 36 h after the occlusion. Brains were removed, and slices were taken. These slices were incubated with fluo-3 solution, and the fluorescent intensity (FI) of $[Ca^{2+}]_i$ was viewed by confocal microscopy. There were significant differences in FI of Ca^{2+} between the ischaemic caudoputamen and the contralateral region in the seven groups of animals ($F = 24.34$, $P < 0.001$), while the difference between the ischaemic frontoparietal cortex and the contralateral region was not significant within 1.5 h of occlusion ($F = 1.06$, $P > 0.05$). Calcium overload occurred prior to an abrupt reduction in ADC in the peripheral ischaemic area. The relative ADC (rADC) and FI (rFI) were negatively correlated in the frontoparietal cortex ($r = -0.9$, $P < 0.001$), but not in the caudoputamen ($r = -0.21$, $P > 0.05$). Our findings suggest that ADC of the perifocal ischaemic area might reflect the changes in intracellular calcium which occur in early ischaemia. They may also suggest that, once the calcium level is high enough and infarction ensues, changes in ADC may not induce a further rise in calcium concentration.

Keywords Cerebral ischaemia · Calcium · Magnetic resonance imaging

Introduction

Diffusion-weighted imaging (DWI) has been found to be more sensitive than conventional T2-weighted imaging (T2WI), both in animals and humans, in detecting early cerebral ischaemia [1, 2, 3]. The decrease in apparent diffusion coefficient (ADC) in early ischaemia is caused by restricted diffusion of water, and is observed as high signal on DWI. This reduction in ADC is believed to reflect cytotoxic oedema and shrinkage in the extracellular volume [4, 5, 6]. The accuracy of DWI in discriminating between potential viable tissue (penumbra) and irreversible infarct has been questioned, however [7, 8, 9], and recent studies have shown that a combination of DWI and perfusion-weighted imaging (PWI) is more effective than DWI alone in pinpointing the penumbra [10, 11, 12, 13, 14, 15].

Calcium homeostasis is important in maintaining normal cell metabolism. Pathways of cell death are thought to involve calcium overload, and calcium-related mechanisms have also been found to cause brain cell injury, in both core and penumbral tissue [16, 17]. Attempts to show that calcium antagonists can act as

neuroprotective drugs, however, have been ambiguous, especially in clinical trials. [18, 19].

To determine the role of intracellular calcium in ischaemic neuronal death, we induced focal regional ischaemia in rabbits by transorbital permanent occlusion of one middle cerebral artery (MCAo). We then assayed changes in ADC, regional cerebral blood flow (CBF) and intracellular calcium concentration ($[Ca^{2+}]_i$) which occur over time in the ischaemic core and peripheral areas, of the rabbit brain.

Materials and methods

This research was approved by the Animal Research Committee of Peking University Health Science Centre. We randomly assigned 42 New Zealand White rabbits weighing 2.5–3.5 kg to seven equal groups. They underwent unilateral permanent occlusion of the MCA for 0.5, 1.5, 3, 6, 12, 24 or 36 h before being studied. The animals were initially anaesthetised with 20% urethane (1 g/kg) by injection into the marginal ear vein. A femoral artery catheter was inserted for continuous monitoring of blood pressure, pH, PaO_2, $PaCO_2$ and glucose. A second catheter was placed in the right femoral vein for administration of drugs and infusion of isotonic saline 3 ml/h throughout the experiment. Body temperature was monitored with a rectal probe and kept near 38.5°C with a warming blanket. Anaesthesia was maintained with pentobarbital sodium (3–5 mg/kg/h). The MCA was exposed through the transorbital approach and permanently occluded just proximal to the perforating arteries using bipolar electrical coagulation, followed by complete transection under an operating microscope [20]. The craniectomy was covered with Gelfoam, then with gauze soaked with isotonic saline. The wound and eyelid were closed with sutures.

Following surgery, each animal was placed supine with its head fixed in a 3-in flexible surface coil. The rabbit was fastened into a custom-built stereotaxic body holder to reduce motion. MRI consisting of DWI and PWI, was performed using a 1.5-Tesla echoplanar imaging (EPI)-capable imager. We acquired three orthogonal interleaved scout images for accurate orientation. Total imaging time was about 6 min.

DWI was performed with an EPI spin-echo sequence (TR 4987 TE 103 ms). We obtained ten coronal slices parallel to the tentorium cerebelli, focused on the optic chiasm, slice thickness 3 mm; interslice gap 0.5 mm, field of view 210 mm, matrix 128×128. A T2-weighted reference image (b 0 s/mm^2) and DWI using a diffusion gradient (b 1000 s/mm^2) applied orthogonally in three directions, were collected.

Perfusion studies were also performed with an EPI spin-echo sequence (TR 1.2 TE 42.1 ms). Five contiguous 3 mm coronal slices, interslice gap 0.5 mm, field of view 230 mm, matrix, 128×128 were designed to match the five DWI slices showing the largest diffusion defects. They were imaged 40 times at intervals of 1.38 s. After four sets of baseline images, a bolus injection of gadolinium diethylene triaminepenta-acetate (GD-DTPA) 0.2 mmol/kg, was given through the intravenous catheter at 0.2 ml/s using a power injector, followed by a 5 ml bolus of isotonic saline at the same rate.

The core of ischaemia was in the lateral caudoputamen, and the final ischaemic lesion involved the residual part of the striatum and its adjacent cortex [20, 21]. Regions of interest (ROI) of about 3 pixels were drawn freehand in the ischaemic caudoputamen, frontoparietal cortex and contralateral anatomical areas; these were used to calculate diffusion and perfusion parameters.

Trace diffusion images were produced by calculating the average of the three diffusion-weighted images. ADC maps were reconstructed on a pixel-by-pixel basis. ADC was calculated using the linear regression formula: $\ln(S/S_0) = -b\,(ADC)$, where S, S_0 are the signal intensities with and without the diffusion-sensitive-gradient, respectively.

Raw perfusion raw images were transferred to an image processor for calculation of CBF, using the model-independent singular value decomposition method. The tissue-concentration curve was deconvolved with the arterial input function by manually choosing one pixel over the MCA of the unaffected hemisphere. The pixel was used only if it showed an early decrease in intensity and a large reduction in intensity on the tissue concentration-time curve compared with normal brain parenchyma.

Relative ADC (rADC) and CBF (rCBF) were also calculated: $rADC\,(rCBF) = ADC\,(CBF)_{ischemia} / ADC\,(CBF)_{contralateral} \times 100\%$.

We chose two axial slices, involving the largest area of DWI defect in the caudoputamen or frontoparietal cortex. Then the vertical dimension (VD) between the selected slice and the top of the cerebrum was measured in the sagittal section, and were used for localisation during the preparation of brain slices.

The animal was killed at the predetermined time after the final imaging. Within 3 min the brain was removed from the cranium and the cerebellum was cut away. The detached brain was rapidly infused for about 5 min in artificial cerebrospinal fluid (ACSF) ventilated with a 95%O_2-5%CO_2 mixture [22]. The cerebrum was divided into two symmetrical halves from the falx cerebri. The ischaemic hemisphere was placed on the platform of the soft-tissue slicing machine underlain with a soaked filter paper. According to the VD obtained from DWI, the tissue in the two selected planes was sliced into three to five $400 \pm 100\mu m$ sheets parallel to the tentorium cerebelli. The nonischaemic hemisphere was treated identically. The yield per rabbit was 12–20 sheets.

A solution containing 15μmol/L fluo-3 acetoxymethyl ester (fluo-3), a membrane-permeable calcium-sensitive fluorescent dye, and 10% (weight/volume) Pluronic F-127 in ACSF was prepared in a light-shielded container and ventilated with 95%O_2-5%CO_2. Brain sheets were immersed in this for 40 min at room temperature and washed three times in ACSF without dyes.

Fluorescence intensity (FI) was measured with a laser scanning confocal microscope with an argon-krypton source. Each specimen was placed in a custom-made container containing a light-permeable bottom cover glass and examined under a 20× oil-immersion lens. Optical sections 10 μm thick were collected at an excitation wavelength of 488 nm, and the distribution of fluo-3 ROI, corresponding to the defects of DWI and the contralateral regions, were imaged. Following gross orientation with the light microscope, the laser transmitter was used to examine five contiguous visual fields in the selected regions of each brain sheet. The intensity of the entire visual field was measured, and two ischaemic and two non-ischaemic ROI were examined. The mean FI in each ROI was determined from the average of 15–25 visual fields in 3–5 brain sheets. All processes were performed as rapidly as possible to reduce further hypoxia which could lead to an overestimation of ischaemia. Since absolute FI could be affected by all the procedures, including time of brain slice preparation, brain thickness, loading temperature, time of fluorescent examination, and attenuation, the relative FI (rFI) was calculated as $r\,FI = FI_{ischaemia} / FI_{contralateral} \times 100\%$.

Values, expressed as mean ± SEM, were analysed with SPSS software. Repeated ANOVA was performed on the physiological data, and one-way ANOVA and Student's t-test were performed to analyse the differences in ROI between the ischaemic and contralateral tissues. The relationship between r FI and r ADC was assessed by correlation analysis. $P < 0.05$ was taken as statistically significant.

Table 1 Physiological variables (mean ± sd) before and after middle cerebral artery occlusion

Variable	Before occlusion	After occlusion (h)						
		0.5	1.5	3	6	12	24	36
PaO_2 (kPa)	12.54 ± 0.71	12.46 ± 0.97	11.38 ± 1.12	12.36 ± 0.75	12.25 ± 0.57	12.41 ± 0.73	13.54 ± 1.32	11.92 ± 0.68
$PaCO_2$ (kPa)	3.68 ± 0.23	4.21 ± 0.38	4.18 ± 0.35	3.86 ± 0.44	4.57 ± 0.31	4.26 ± 0.54	3.87 ± 0.86	3.81 ± 0.65
pH	7.29 ± 0.04	7.22 ± 0.14	7.67 ± 0.08	7.37 ± 0.15	7.38 ± 0.29	7.86 ± 0.36	8.05 ± 0.85	7.37 ± 0.38
Glucose (mmol/l)	7.34 ± 0.5	7.27 ± 0.8	7.27 ± 0.7	7.76 ± 0.2	7.37 ± 0.5	7.58 ± 0.4	7.93 ± 0.8	7.21 ± 0.7
Temperature °C	39.2 ± 0.6	38.1 ± 0.5	37.8 ± 0.7	38.7 ± 0.9	38.9 ± 0.4	39.1 ± 0.8	39.7 ± 0.6	38.2 ± 0.7
Observations		42	36	30	24	18	12	6

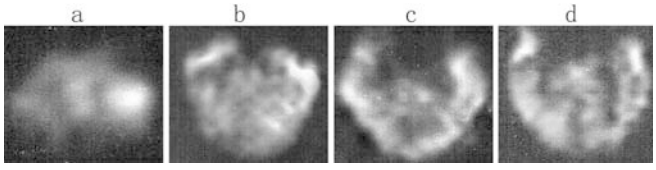

Fig. 1a–d Four contiguous diffusion-weighted images (DWI) (b 1000 s/mm^2) 30 min after middle cerebral artery occlusion (MCAo). High signal appeared in the left caudoputamen (↑)

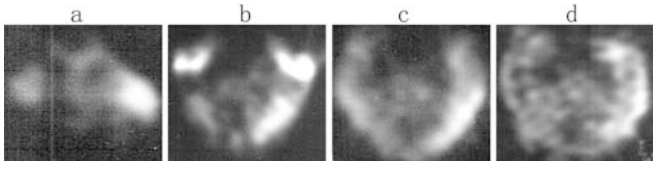

Fig. 2a–d Same rabbit as in Fig. 1, 6 h after MCAo, four contiguous DWI were obtained. High signal extended to the left frontoparietal cortex (↑)

Results

Throughout these experiments, the physiological parameters (blood pressure, arterial pH, PaO_2, $PaCO_2$ and glucose) of each animal remained within the normal range (Table 1). There were no significant differences between the pre- and postoperative values ($P > 0.05$, ANOVA).

We saw increased signal on DWI 30 min after MCAo in the caudoputamen of the affected side (Fig. 1) in 38 rabbits (90.5%) and in the adjacent frontotemporal cortex in four (9.5%). High signal appeared 90 min after MCAo in the caudoputamen of the remaining animals, but there was no evidence of ischaemia in the T2-weighted images. The area of abnormal intensity on DWI images increased relative to the ischaemia, high signal gradually appearing in the left frontoparietal cortex 3–6 h after the occlusion (Fig. 2).

In the caudoputamen of the affected side (ischaemic core), ADC decreased markedly within 6 h of occlusion (Table 2). From 12 to 36 h, ADC in this area gradually increased, but remained below normal. The difference between ischaemic and contralateral measurements was significant ($F = 86.48$, $P < 0.001$).

In the ischaemic frontoparietal cortex ADC gradually decreased, but there was no significant difference between ischaemic and contralateral parameters up to 3 h after occlusion ($F = 2.04$, $P > 0.05$). From 6 h after the occlusion, however, the reduction in ADC was significant ($F = 75.94$, $P < 0.001$).

From 30 min to 6 h after MCAo, r ADC of the caudoputamen was significantly lower than that of the frontoparietal cortex ($F = 103.48$, $P < 0.001$). However,

Table 2 Apparent diffusion coefficients (ADC, ×10^{-5} mm^2/s) and cerebral blood flow (CBF, ml/100g/min) for regions of interest in the ischaemic and contralateral hemispheres

Time after occlusion (h)	Caudoputamen				Frontoparietal cortex			
	ADC		CBF		ADC		CBF	
	Ischaemic	Contralateral	Ischaemic	Contralateral	Ischaemic	Contralateral	Ischaemic	Contralateral
0.5	0.43 ± 0.11	0.80 ± 0.18	16.4 ± 3.2	59.7 ± 4.1	0.77 ± 0.16	0.83 ± 0.13	30.9 ± 5.9	64.6 ± 5.9
1.5	0.37 ± 0.13	0.81 ± 0.26	9.3 ± 1.3	53.8 ± 4.5	0.71 ± 0.13	0.85 ± 0.19	22.9 ± 5.8	69.1 ± 7.5
3	0.36 ± 0.12	0.82 ± 0.12	9.7 ± 2.3	60.8 ± 5.7	0.69 ± 0.17	0.84 ± 0.13	14.3 ± 4.9	61.9 ± 6.4
6	0.34 ± 0.16	0.81 ± 0.15	10.2 ± 2.6	59.4 ± 6.6	0.45 ± 0.19	0.86 ± 0.11	15.8 ± 6.1	67.7 ± 7.8
12	0.37 ± 0.17	0.82 ± 0.11	10.7 ± 2.1	55.1 ± 5.4	0.36 ± 0.09	0.82 ± 0.11	15.6 ± 5.8	64.5 ± 6.6
24	0.38 ± 0.14	0.80 ± 0.09	12.4 ± 2.9	54.6 ± 6.1	0.38 ± 0.10	0.82 ± 0.12	24.4 ± 4.9	63.8 ± 5.2
36	0.43 ± 0.16	0.82 ± 0.13	14.8 ± 1.3	56.1 ± 6.2	0.49 ± 0.11	0.84 ± 0.17	27.9 ± 6.8	66.1 ± 5.9

There were significant differences ($P < 0.001$, paired-samples t-test) between ROI in the ischaemic and contralateral hemispheres of at each time point except for ADC in the cortex up to 3 h ($P > 0.05$)

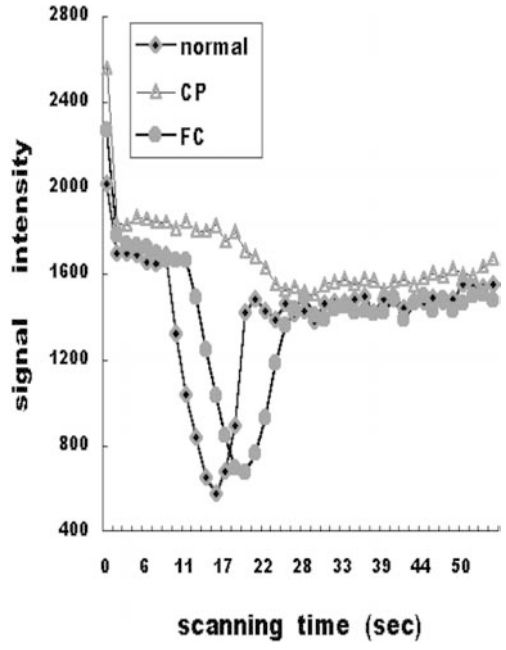

Fig. 3 Temporal changes in signal intensity in the ischaemic caudoputamen (CP, Δ) and frontoparietal cortex (FC, ●), and contralateral nonischaemic tissue (Normal, ◆) 30 min after MCAo

after 12 h, this difference was no longer significant ($F = 0.66$, $P > 0.05$).

Perfusion deficits involving the entire MCA were observed 30–90 min after occlusion. As shown by signal intensity changes during the bolus passage in the ROI, a well-defined first pass was observed in the nonischaemic hemisphere, while the maximum signal reduction decreased and the time-to-peak was delayed in the peripheral ischaemic region, without a first-pass effect in the ischaemic caudoputamen (Fig. 3). On the ischaemic side, the mean CBF ranged from 9.3 to 16.4 ml/100g/min in the caudoputamen and from 14.3 to 30.9 ml/100g/min in the frontoparietal cortex (Table 2). *r* CBF in the caudoputamen was 12.36% 3 h after the occlusion, 13.69% after 6 h and 25.75% after 36 h, while *r* CBF in the frontoparietal cortex was 23.71% after 3 h, 27.05% after 6 h and 37.13% after 36 h. The difference in *r* CBF between the caudoputamen and frontoparietal cortex was significant ($F = 14.94$, $P < 0.001$).

In the seven groups of rabbits, there were no significant differences in FI of Ca^{2+} in the caudoputamen ($F = 0.59$, $P > 0.05$) and frontoparietal cortex ($F = 0.71$, $P > 0.05$) of the nonischaemic hemisphere. However, there were significant differences overall between the ischaemic and contralateral caudoputamen in these groups of animals ($F = 24.34$, $P < 0.001$) (Fig. 4). While the difference between the ischaemic frontoparietal cortex and the contralateral region was not significant within 1.5 h of the occlusion ($F = 1.06$, $P > 0.05$), it became so 3–36 h after surgery ($F = 5.19$, $P < 0.01$) (Fig. 4). The *r* FI of the caudoputamen was significantly higher than that of the frontoparietal cortex until 24 h after MCAo, but not at 36 h (Fig. 5). *r* ADC and *r* FI were negatively correlated in the frontoparietal cortex ($r = -0.9$, $P < 0.001$), but there was no significant correlation in the caudoputamen ($r = -0.14$, $P > 0.05$) (Fig. 6).

Discussion

While most studies of Ca^{2+} metabolism during ischaemic injury have been performed in cell culture models [23], we used an in vivo focal ischaemic model, in which DWI and PWI techniques were combined with measurements of $[Ca^{2+}]_i$, to study the correlation between Ca^{2+} metabolism and ischaemic injury. The measurements of $[Ca^{2+}]_i$ at the tissue level better approximated the pathophysiology observed in stroke, suggesting that this method may be appropriate for localisation and quantitative analysis in ischaemic injury.

Fig. 4 Fluo-3 fluorescent images of rabbit brain slice 0.5, 1.5, 3, 6, 12, 24 and 36 h after MCAo were obtained. One visual field of the ischaemic caudoputamen (CP, *top*) and frontoparietal cortex (FC, *bottom*), original magnification ×20

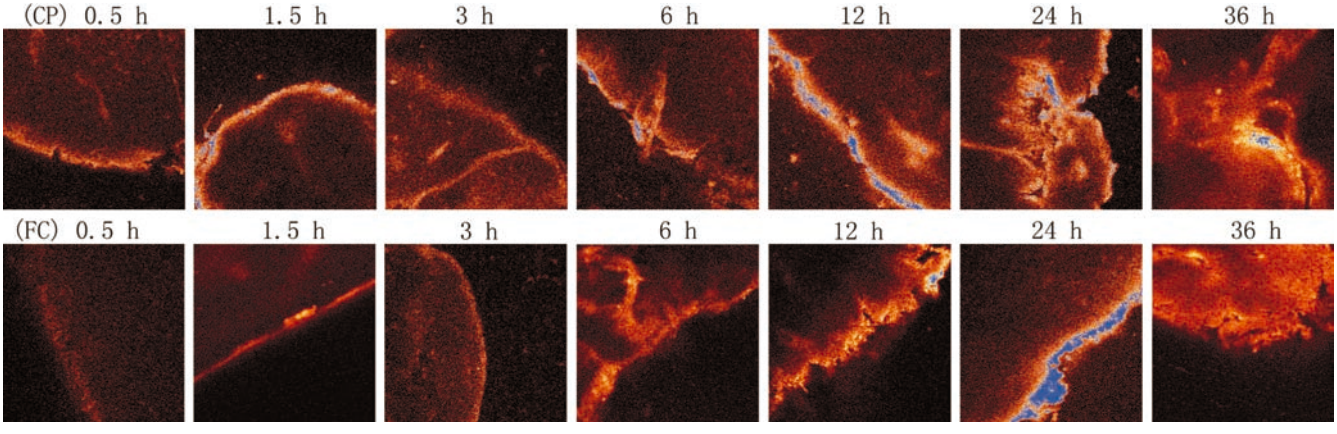

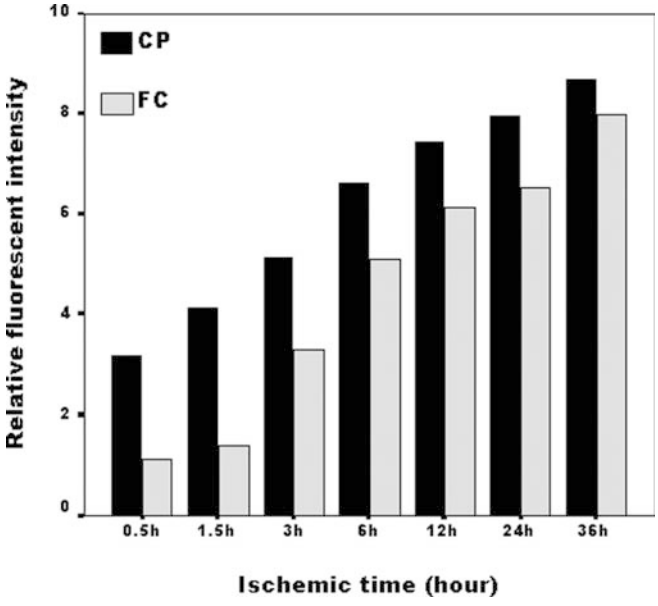

Fig. 5 Relative FI (rFI) of Ca^{2+} in the caudoputamen (CP) and frontoparietal cortex (FC). rFI of CP was significantly higher than that of FC within 24 h of occlusion, but there was no significant difference between them at 36 h. (∇ $P < 0.01$ ▲ $P < 0.05$ ● $P > 0.05$)

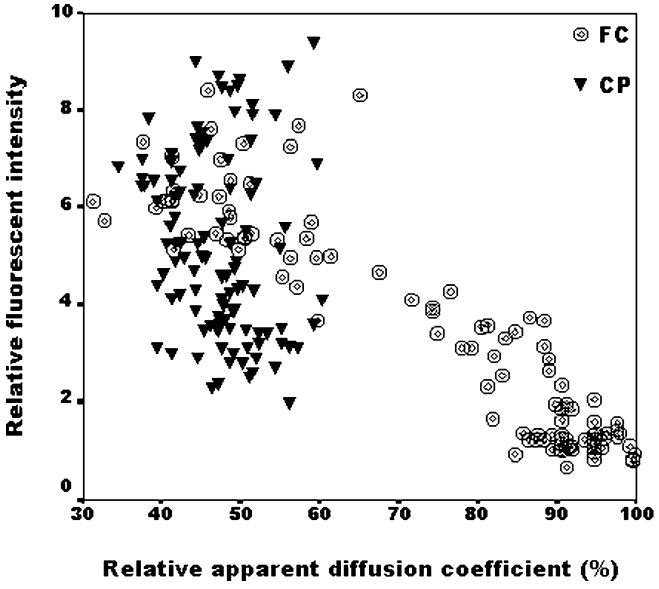

Fig. 6 Relationship between relative fluorescent intensity (rFI) and relative apparent diffusion coefficient (rADC) of frontoparietal cortex (FC, ▮) and caudoputamen (CP, ▼), respectively

Within 36 h of MCAo, ADC goes through a process of dynamic change. Among the mechanisms that may contribute to ADC reduction [24] are reduction in extracellular space, an increase in the viscidity and tortuosity of the extracellular space; a decrease in capillary vessel perfusion and local hypothermia, caused by blood-flow reduction or cessation; and an increase of intracellular viscidity and a decrease of cytoplasmic flow resulting from the collapse of the cytoskeleton. Although the methods have not been delineated, ADC reduction is believed to be related to energy failure and tissue injury [25, 26, 27]. The gradual increase in ADC observed at the terminus of acute and subacute ischaemia may be due to cytotoxic oedema or cell collapse, colliquation [28].

During early ischaemia, we observed changes in rADC and rCBF in the ischaemic frontoparietal cortex; rCBF decreased markedly ($< 46\%$) but rADC only mildly ($> 80\%$) within 3 h of occlusion. This region, called the DWI/PWI mismatch, is thought to represent the ischaemic penumbra [10, 11, 12, 13, 14, 15]. In these penumbral regions, defined as the areas surrounding the severe ischaemic lesion, cells are in state of 'electrical silence' and may recover if reperfusion and neuroprotective drugs are applied in time [29]. This area may have a more abundant collateral blood supply than the basal ganglia in the more vulnerable end-arterial area. Our finding that ADC fell significantly in the ischaemic cortex 6 h after the occlusion, despite the persistent reduction in CBF, suggests that the decrease in ADC is also related to the duration of ischaemia [30].

We observed calcium overload in both the ischaemic core and the peripheral area. $[Ca^{2+}]_i$ in the ischaemic core increased immediately after MCAo and was elevated throughout, supporting the concept that massive, rapid influx of Ca^{2+} is a major mediator of ischaemic cell death in the core region of complete ischaemia, [30]. We also found that $[Ca^{2+}]_i$ of the perifocal area remained normal within 1.5 h of MCAo, whereas CBF was significantly reduced, suggesting that, although perfusion of the perifocal tissue was subnormal during the early stages of ischaemia, these cells could maintain basal metabolism and ion and water homeostasis.

We also found that calcium overload occurred prior to the abrupt reduction in ADC in the peripheral ischaemic area. There is evidence that a lasting perturbation of the plasma membrane, resulting from a sustained low perfusion, leads to intracellular calcium accumulating slowly, but not rapidly, and when $[Ca^{2+}]_i$ reaches a certain level, which exceeds the ability of the mitochondria, massive and rapid influx of calcium will occur. Apoptosis is believed to be triggered by gradual accumulation of intracellular calcium, combined with mitochondrial dysfunction [32].

We observed a significant correlation between $[Ca^{2+}]_i$ and ADC reduction in the peripheral ischaemic region, but not in the caudoputamen. The reasons are not clear. It may be due to dysfunction of the cell membrane, which may lead to a massive influx of calcium ions and water molecules. It may suggest that ADC in the perifocal ischaemic region might reflect the changes in

intracellular calcium in early ischaemia. A lack of association in the ischaemic core might suggest that, once the calcium level is high enough, infarction ensues; thus, there would be no relationship between further elevation in the calcium concentration and changes in the diffusion coefficient.

While our results are of considerable interest, our study has several drawbacks. First, the measurement intervals were relatively broad, precluding our noting changes in calcium metabolism and ADC immediately after the ischaemic insult. Second, we did not perform electron microscopy on these samples, which would yield more sensitive methods data on the morphological changes occurring during the ischaemic process. Third, by performing an initial craniotomy, we lost the cerebrospinal fluid. And finally, although our model is useful for studying ischaemic changes, it does not allow for intervention.

Although calcium antagonists have been shown to reduce the area of an infarct and to improve prognosis in animal ischaemic models, the results have proved equivocal in clinical experiments. Our observations on the changes in ADC in acute stroke suggest that intracellular calcium may accumulate in the perifocal ischaemic lesion. This would provide new, practical guidelines for MRI values, both DWI and PWI, which would enable clinicians to design therapeutic regimes and to monitor patients suffering from acute stroke.

Acknowledgements This research was funded by National Natural Science Foundation of China (39900034).

References

1. Moseley ME, Cohen Y, Mintorovitch J (1990) Early detection of regional cerebral ischemia in cats: comparison of diffusion- and T2-weighted MRI and spectroscopy. Magn Reson Med 14:330–346
2. Warach S, Gaa J, Siewert B, Wielopolski P, Edelman RR (1995) Acute human stroke studied by whole brain echo planar diffusion-weighted magnetic resonance imaging. Ann Neurol 37:231–241
3. Ay H, Buonanno FS, Rordorf G (1999) Normal diffusion-weighted MRI during stroke-like deficits. Neurology 52:1784–1792
4. Van Bruggen N, Roberts TP, Cremer JE (1994) The application of magnetic resonance imaging to the study of experimental cerebral ischaemia. Cerebrovasc Brain Metab Rev 6: 180–210
5. Benveniste H, Hedlund LW, Johnson GA (1992) Mechanism of detection of acute cerebral ischemia in rats by diffusion-weighted magnetic resonance microscopy. Stroke 23: 746–754
6. Le Bihan D, Moonen CT, Van Zijl PC, Pekar J, DesPres D (1991). Measuring random microscopic motion water in tissues with MR imaging: a cat brain study. J Comput Assist Tomogr 15: 19–25
7. Kohno K, Hoehn-Berlage M, Mies G, Back T, Hossmann KA (1995) Relationship between diffusion-weighted MR images, cerebral blood flow, and energy state in experimental brain infarction. Magn Reson Imaging 13: 73–80
8. Minematsu K, Hasegawa Y, Yamaguchi T (1995) Diffusion MRI for evaluating cerebrovascular disease. Rinsho-Shinkeigaku 35: 1575–1577
9. Ueda T, Yuh WT, Taoka T (1999) Clinical application of perfusion and diffusion MR imaging in acute ischemic stroke. J Magn Reson Imaging 10: 305–309
10. Warach S, Dashe JF, Edelman RR (1996) Clinical outcome in ischemic stroke predicted by early diffusion-weighted and perfusion magnetic resonance imaging: a preliminary analysis. J Cereb Blood Flow Metab 16: 53–59
11. Van-Dorsten FA, Hata R, Maeda K(1999) Diffusion- and perfusion-weighted MR imaging of transient focal cerebral ischemia in mice. NMR Biomed 12: 525–534
12. Carano RA, Li F, Irie K (2000) Multispectral analysis of the temporal evolution of cerebral ischemia in the rat brain. J Magn Reson Imaging 12: 842–858
13. Jacobs MA, Zhang ZG, Knight RA (2001) A model for multiparametetric MRI tissue characterization in experimental cerebral ischemia with histological validation in rat: part 1. Stroke 32: 943–949
14. Oliveira-Filho J, Koroshetz WJ (2000) Magnetic resonance imaging in acute stroke: clinical perspective. Topics Magn Reson Imaging 11: 246–258
15. Schlaug G, Benfield A, Baird AE (1999) The ischemic penumbra: operationally defined by diffusion and perfusion MRI. Neurology 53: 1528–1537
16. Kristian T, Siesjo BK (1998) Calcium in ischemic cell death. Stroke 29: 705–718
17. Wang C, Nguyen HN, Maguire JL, Perry DC (2002) Role of intracellular calcium stores in cell death from oxygen-glucose deprivation in a neuronal cell line. J Cereb Blood Flow Metab 22: 206–214
18. Yepes MS (2001) Thrombolytics and neuroprotective agents in the treatment of the patient with an acute cerebrovascular ischemic accident. Rev Neurol 32: 259–266
19. Macdonald RL, Stoodley M (1998) Pathophysiology of cerebral ischemia. Neurol Med Chir 38: 1–11
20. Yamamoto K, Yoshimine T, Yanagihara T (1985) Cerebral ischemia in rabbit: a new experimental model with immunohistochemical investigation. J Cereb Blood Flow Metab 5: 529–536
21. DeLaPaz RL, Shibata D, Steinberg GK (1991). Acute cerebral ischemia in rabbits: correlation between MR and histopathology. AJNR 12: 89–95
22. Xing H, He QH, Yuan L (1999) The experimental study on spatiotemporal changes of intracellular Ca^{2+} in neurons during focal ischemia/reperfusion damage. Chin J Histochem Cytochem 8: 51–56
23. Choi DW (1995) Calcium: still center-stage in hypoxic-ischemic neuronal death. Trends Neurosci 18: 58–60
24. Desmond PM, Lovell AC, Rawlinson AA (2001) The value of apparent diffusion coefficient maps in early cerebral ischemia. AJNR 22: 1260–1267

25. Liu KF, Li F, Tatlisumak T (2001) Regional variations in the apparent diffusion coefficient and the intracellular distribution of water in rat brain during acute focal ischemia. Stroke 32: 1897–1905
26. Davis D, Ulatowski J, Eleff S (1994) Rapid monitoring of changes in water diffusion coefficients during reversible ischemia in cat and rat brain. Magn Reson Med 31: 454–460
27. Mintorovitch J, Yang GY, Shimizu H, Kucharczyk J, Chan PH, Weinstein PR (1994) Diffusion-weighted magnetic resonance imaging of acute focal cerebral ischemia: comparison of signal intensity with changes in brain water and Na^+, K^+-ATPase activity. J Cereb Blood Flow Metab 14: 332–336
28. Pierpaoli C, Righini A, Infante IL (1993) Histopathologic correlation of abnormal water diffusion in cerebral ischemia: diffusion-weighted imaging and light electron microscopic study. Radiology 189: 434–448
29. Back T (1998) Pathophysiology of the ischemic penumbra-revision of a concept. Cell Mol Neurobiol 18: 621–638
30. Wang Y, Hu W, Perez Trepichio AD (2000) Brain tissue sodium is a ticking clock telling time after arterial occlusion in rat focal cerebral ischemia. Stroke 31: 1386–1392
31. Nagasawa H, Kogure K (1990) Exofocal postischemic neuronal death in the rat brain. Brain Res 524: 196–202
32. Dietrich WD (1992) The importance of brain temperature in cerebral injury. J Neurotrauma 9: S475-S485